

## Weighing The Options: The Unseen Companion in LAMOST J2354 is Likely a Massive White Dwarf

M. A. TUCKER,<sup>1,2,\*</sup> A. J. WHEELER,<sup>2</sup> D. M. ROWAN,<sup>2,1</sup> AND M. E. HUBER<sup>3</sup>

<sup>1</sup>*Center for Cosmology and AstroParticle Physics, 191 W Woodruff Ave, Columbus, OH 43210*

<sup>2</sup>*Department of Astronomy, The Ohio State University, 140 W 18th Ave, Columbus, OH 43210*

<sup>3</sup>*Institute for Astronomy, University of Hawai'i, 2680 Woodlawn Drive, Honolulu HI 96822*

Submitted to *The Open Journal of Astrophysics*

### ABSTRACT

LAMOST J235456.73+335625.9 (J2354) is a binary system hosting a  $\sim 0.7 M_{\odot}$  K dwarf and a  $\sim 1.4 M_{\odot}$  dark companion, supposedly a neutron star, in a 0.48 d orbit. Here we present high- and low-resolution spectroscopy to better constrain the properties of the system. The low-resolution spectrum confirms that the luminous star is a slightly metal-poor K dwarf and strengthens the limits on any optical flux from the dimmer companion. We use the high-resolution spectra to measure atmospheric parameters ( $T_{\text{eff}}$ ,  $\log g$ ,  $[\text{Fe}/\text{H}]$ ,  $v_{\text{rot}} \sin i$ ) and abundances for 8 elements for the K dwarf. We refine the mass of the compact object to  $M_{\text{co}} \sim 1.3 M_{\odot}$  with a minimum mass of  $M_{\text{co,min}} = 1.23 \pm 0.04 M_{\odot}$ . The expected overabundance of intermediate-mass elements from the incident supernova ejecta is not detected in the K dwarf atmosphere. This contrasts with known binaries hosting neutron stars where almost all companions show evidence for polluting material. Moving the neutron-star progenitor further from the K-dwarf at the time of explosion to minimize atmospheric pollution requires a finely-tuned kick to produce the current orbital separation of  $\sim 3.3 R_{\odot}$ . Instead, we find that a massive white dwarf with a cooling age of  $\gtrsim 3$  Gyr satisfies all observational constraints. The system likely experienced two common-envelope phases leading to its current state because the white dwarf progenitor was massive enough to ignite He-shell burning. The system will become a cataclysmic variable in the distant future when the K-dwarf evolves off of the main sequence. These short-period high- $q$  binaries represent an intriguing formation pathway for compact double white dwarf binaries and thermonuclear supernovae. An ultraviolet spectrum is the most promising avenue for directly detecting the white dwarf companion.

*Keywords:* Close binary stars (254), White dwarf stars (1799), Common envelope evolution (2154), Low mass stars (2050), Stellar abundances (1577)

### 1. INTRODUCTION

Massive white dwarfs (WDs) are the remnants of  $6 - 8 M_{\odot}$  zero-age main sequence (ZAMS) stars. These stars are rare, confirmed by the rarity of massive WDs (e.g., Kilic et al. 2021), but represent a key contributor of nucleosynthetic material to the interstellar medium (ISM). A single  $\sim 7 M_{\odot}$  star contributes the same amount of material to the ISM as  $\sim 20$   $1-M_{\odot}$  stars (Cummings et al. 2018). The core composition of massive WDs traces which elements were fused during stellar evolution. Stars with  $M_{\text{ZAMS}} \sim 8 - 12 M_{\odot}$  can ignite carbon but not neon in the core, producing

O+Ne+Mg WDs instead of the C/O WDs that originate from stars with  $M_{\text{ZAMS}} \sim 0.5 - 8 M_{\odot}$  (e.g., Camisassa et al. 2019). Characterizing these stellar remnants constrains relativistic effects in degenerate plasmas (Althaus et al. 2023), traces the star-formation of the Milky Way (Fantin et al. 2019), and reveals the chemical composition of post-MS planetary systems (Jenkins et al. 2024).

Yet these intermediate-mass stars that become massive WDs prefer companionship, with more than half having a companion close enough for mass-transfer during their evolution (Moe & Di Stefano 2017). This will affect the long-term evolution of both stars, complicating reliable comparisons to WD cooling models. Close binaries will almost always experience a common-

\* CCAPP Fellow

envelope (CE) phase where the lower-mass star becomes embedded in the extended, tenuous envelope of the more massive star as it evolves through the giant branch (see Röpke & De Marco 2023 for a recent review). CE interaction results in the expulsion of the envelope and orbital decay, producing tight binaries which are the precursors for stellar mergers, supernova progenitors, and X-ray binaries. Despite the ubiquity of CE phases in binary stellar evolution and its wide-ranging influence across astrophysical disciplines, we have only a crude understanding of the physical processes determining the final outcome(s) (e.g., Ivanova 2011; Postnov & Yungelson 2014; Marchant et al. 2021).

Discovering and characterizing post-CE binaries remains the most promising avenue for empirically constraining the underlying physics (e.g., Zorotovic et al. 2010; Zorotovic & Schreiber 2022; Scherbak & Fuller 2023; Belloni et al. 2024; Yamaguchi et al. 2024a). Yet discovering these systems is complicated by the small sizes and inherently low luminosities of WDs, especially since even low-mass K and M dwarfs can outshine the WD at optical and infrared (IR) wavelengths (e.g., Rebassa-Mansergas et al. 2021). Identifying WDs with non-degenerate companions was historically biased towards accreting systems, such as cataclysmic variables (CVs), because accretion produces luminous emission spanning the electromagnetic spectrum (e.g., Ritter & Kolb 2003; Barlow et al. 2006; Drake et al. 2014; Schwöpe et al. 2024). This is shifting in the era of astrometry and parallaxes from the *Gaia* mission which has revolutionized the discovery of WDs in wider binaries (e.g., Shahaf et al. 2024; Yamaguchi et al. 2024b).

Yet there exists a subset of quiescent WD+main sequence (MS) binaries with small separations ( $a \lesssim 100 R_{\odot}$ ). They are not close enough to drive accretion but too close for *Gaia* to detect photocenter variability from the orbital motion. Lower-mass WDs have larger radii and thus higher luminosities, increasing their chances of detection (e.g., Kosakowski et al. 2020). There is also a bias towards red companions (i.e., M dwarfs) as each star contributes similar luminosities at different wavelengths (e.g., Rebassa-Mansergas et al. 2012). More difficult to find are the smaller and more massive WDs, which also cool faster than their lower-mass counterparts (Bédard et al. 2020; Camisassa et al. 2022). Careful analyses of astrometric, spectroscopic, and photometric observations are typically required to confidently identify these systems (e.g., Rowan et al. 2024b).

Further complicating the search for massive WDs in quiescent binaries is the overlap between massive WDs ( $< 1.4 M_{\odot}$ ; Takahashi et al. 2013) and low-mass neutron

stars (NSs,  $\gtrsim 1.2 M_{\odot}$ ; Özel et al. 2012; Suwa et al. 2018). Young NSs can typically be identified in radio or X-ray observations (e.g., Manchester et al. 2005; Yang et al. 2017) and young WDs are often hot ( $T_{\text{eff}} \gtrsim 10^4$  K) making them bright in the ultraviolet (UV; e.g., Gray et al. 2011; Garbutt et al. 2024). Older systems with slowly-spinning NSs or cool WDs have limited options for conclusively determining the nature of a  $\sim 1.2 - 1.4 M_{\odot}$  unseen companion to a more luminous MS star.

Finding stars with large radial velocity (RV) variations remains a promising avenue for detecting quiescent compact objects (e.g., Jayasinghe et al. 2023; Liu et al. 2024; Rowan et al. 2024a). Zheng et al. (2023, hereafter Z23) recently reported the discovery of LAMOST J235456.73+335625.9 (J2354), a nearby ( $d = 127.7 \pm 0.3$  pc) K dwarf with a  $\sim 1.4 - 1.6 M_{\odot}$  unseen companion in a  $\sim 0.48$  d orbit. They favor a NS companion but note that a massive WD cannot be fully excluded. After its discovery, we obtained follow-up spectroscopy of J2354 to refine the inferred masses and search for polluting ejecta in the K dwarf atmosphere. Here we find that the unseen companion is more likely to be a massive WD instead of a NS. The data reduction and calibration are described in §2. We measure atmospheric parameters ( $T_{\text{eff}}$ ,  $\log g$ ,  $[\text{Fe}/\text{H}]$ ,  $v_{\text{rot}} \sin i$ ) and the abundances of 8 elements for the K dwarf in §3. We show in §4 that a massive WD is more plausible than a low-mass NS based on available observations. Finally, §5 summarizes our results.

## 2. SPECTROSCOPIC OBSERVATIONS

We obtained low-resolution and high-resolution follow-up spectroscopic observations of J2354 after its discovery. The low-resolution spectrum was obtained by the SuperNova Integral Field Spectrograph (SNIFS; Lantz et al. 2004) on the UH2.2m telescope through the Spectroscopic Classification of Astronomical Transients (SCAT; Tucker et al. 2022) survey. The spectrum covers  $\approx 3400 - 9000 \text{ \AA}$  at a resolution of  $R \approx 1200$ .

Three high-resolution spectra were obtained with the Potsdam Echelle Polarimetric and Spectroscopic Instrument (PEPSI; Strassmeier et al. 2015, 2018) on the Large Binocular Telescope (LBT). We used the  $200 \mu\text{m}$  fiber yielding a resolution of  $R \approx 130,000$  ( $\Delta v \approx 2.3 \text{ km s}^{-1}$ ). The CD2 and CD4 dispersers were used to cover  $4300 - 4800 \text{ \AA}$  and  $5500 - 6300 \text{ \AA}$  simultaneously. We measure and report radial velocities (RVs) for both channels in Appendix A but only the red channel is used for determining stellar parameters. K dwarf spectra are line-blanketed at blue ( $\lesssim 5500 \text{ \AA}$ ) wavelengths, rendering the continuum difficult to constrain. Attempts to include both channels in fitting the atmo-

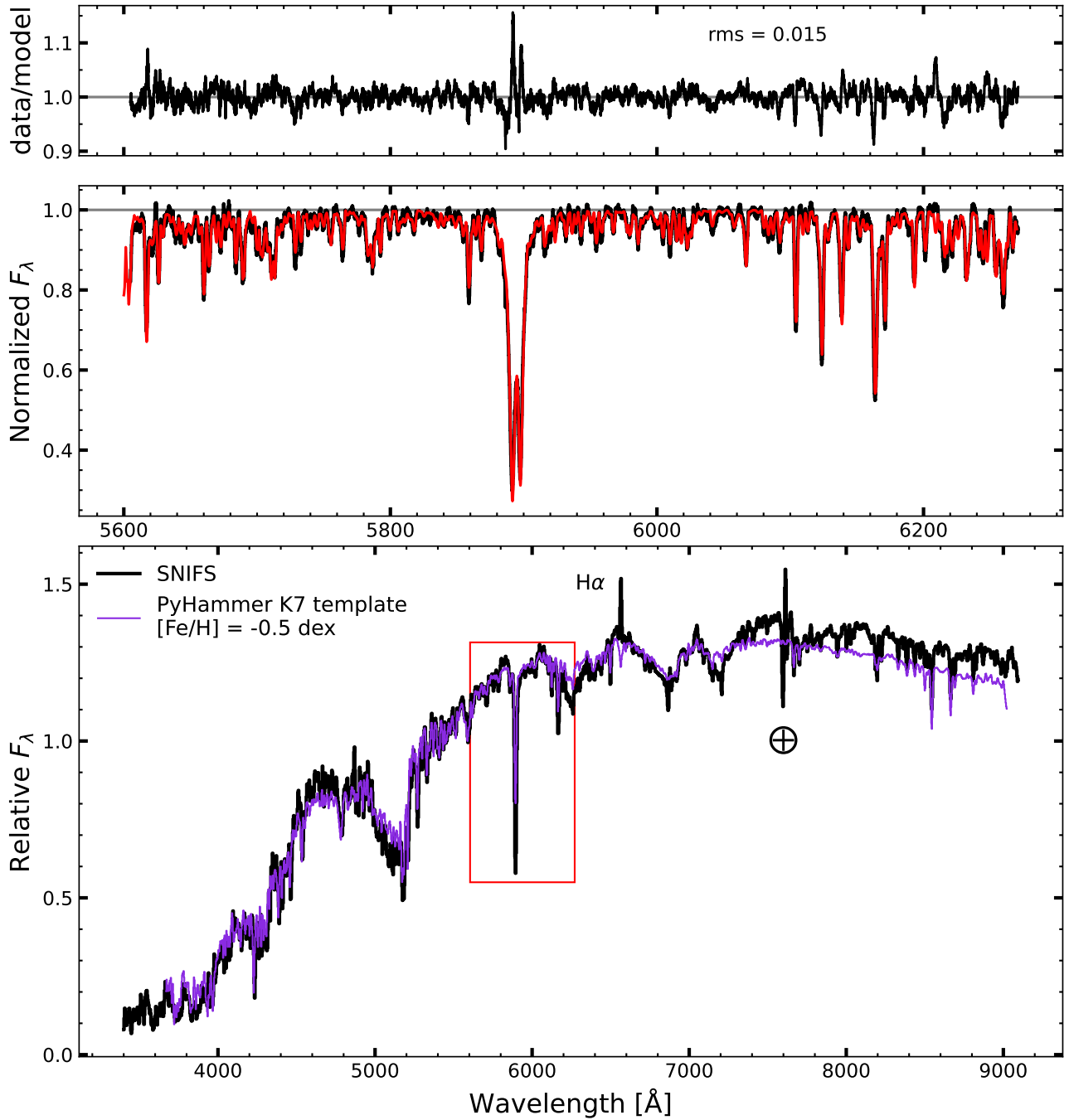


**Figure 1.** Spectroscopic observations of J2354. The bottom panel shows the  $R \sim 1200$  SNIFS spectrum compared to the best-match  $[M/H] = -0.5$  dex PyHammer (Kesseli et al. 2017; Roulston et al. 2020) K7V template (purple), convolved and re-binned to the SNIFS resolution. The red rectangle shows the wavelength coverage of the  $R \approx 130,000$  PEPSI spectrum shown in the middle panel. The best-fit atmospheric model is overlaid in red and the residuals are shown in the top panel. The PEPSI spectrum and residuals have been re-binned to  $0.1 \text{ \AA}/\text{pixel}$  for visual clarity.

Parameter	Value	$\sigma_{\text{sys}}$	$\sigma_{\text{obs}}$	$\sigma_{\text{tot}}$	Unit
$T_{\text{eff}}$	4327	100	11	101	K
$\log g$	4.66	0.20	0.082	0.22	dex
[M/H]	-0.48	0.10	0.026	0.10	dex
$v_{\text{rot}} \sin i$	70.3	2.7	2.8	3.9	km s <sup>-1</sup>

**Table 1.** The adopted stellar parameters and uncertainties based on the high-resolution PEPSI observations. See text for details.

spheric parameters was unsuccessful. Using only the red channel also allows us to ignore potential contamination at blue wavelengths from a WD or low-luminosity accretion disk.

### 3. PROPERTIES OF THE K DWARF

#### 3.1. Bulk Properties

Fig. 1 shows the spectra of J2354. We use PyHammer (Kesseli et al. 2017; Roulston et al. 2020) to compare the low-resolution spectrum against a library of templates. The best-matching template is a metal-poor ([Fe/H] = -0.5 dex) K7 dwarf which we use to initialize the stellar parameters when fitting the high-resolution spectrum below. We adopt the photo-geometric distance of  $d = 127.3 \pm 0.3$  pc from Bailer-Jones (2023) and negligible interstellar reddening based on the dust maps of Green et al. (2019) to remain consistent with Z23.<sup>1</sup>

We analyze the high-resolution PEPSI spectrum using the `fit_spectrum` function in the Korg (Wheeler et al. 2023, 2024) spectral synthesis package. First, we simultaneously fit  $T_{\text{eff}}$ ,  $\log g$ , [M/H], and  $v_{\text{rot}} \sin i$  to the normalized PEPSI spectrum. The empirical continuum normalization is imperfect, so we include minor continuum corrections after the first fit and re-fit with the adjusted continuum (the change this causes in the inferred values is smaller than both the statistical and systematic error). The linelist was obtained from the “extract stellar” mode of the Vienna Atomic Line Database (VALD; Piskunov et al. 1995; Ryabchikova et al. 2015).<sup>2</sup> The linelist references can be found in Appendix A.

The high signal-to-noise ( $\sim 100$ ) and spectral resolution ( $R \sim 130,000$ ) of the PEPSI spectra make the systematic uncertainties dominant over statistical ones.

<sup>1</sup> The more recent 3D dust maps of Dharmawardena et al. (2024) predict a non-negligible extinction of  $A_V = 0.12^{+0.05}_{-0.04}$  mag. This does not affect the interpretation of J2354 besides a slight increase to the UV excess.

<sup>2</sup> The “extract stellar” mode is designed to provide all known spectral features in the specified  $\lambda$  range for a given set of stellar parameters. Note that VALD includes both atomic and molecular lines.

These systematics include physical uncertainties in stellar atmosphere models, computational shortcuts in radiative transfer modeling (i.e., LTE), and instrumental/observational effects such as orbital smearing. For  $T_{\text{eff}}$ ,  $\log g$ , and [M/H] we estimate systematic uncertainties of 100 K, 0.2 dex, and 0.1 dex based on Jofré et al. (2019) and Hegedűs et al. (2023). We propagate these uncertainties to rotation by refitting for  $v_{\text{rot}} \sin i$  with each parameter perturbed in each direction by its assumed systematic uncertainty and adding the perturbations to  $v_{\text{rot}} \sin i$  in quadrature. The uncertainty in [M/H] dominates the systematic uncertainties in  $v_{\text{rot}} \sin i$ .

Individual fits to the three 40-minute exposures provide stellar parameters very close to those from the stacked-spectrum fit, but with dispersions slightly larger than the statistical errors on the parameters. We adopt the sample standard deviation among the visits as the measurement error for each parameter. Measurement of  $v_{\text{rot}} \sin i$  is complicated by potential orbital smearing during the 40-minute exposures. The orbital ephemeris specified by Z23 suggests the spectra span orbital phases of  $\phi \approx 0.2 - 0.4$ <sup>3</sup> where radial acceleration is minimal, and the period uncertainty of  $10^{-5}$  d corresponds to a phase uncertainty of  $\delta\phi \approx 0.1$ . In order to better account for orbital smearing, we adopt the SNR-weighted average of the  $v_{\text{rot}} \sin i$  values from each fit, which is 2.9 km s<sup>-1</sup> lower than that from the stacked spectrum.

The final atmospheric parameters and adopted uncertainties are provided in Table 1. Our values generally agree with those published by Z23 within uncertainties.<sup>4</sup> Overall, the luminous star is a rapidly-rotating metal-poor K-dwarf. We estimate  $M_{\star} = 0.61 \pm 0.04 M_{\odot}$  and  $R_{\star} = 0.65 \pm 0.03 R_{\odot}$  by fitting the derived  $T_{\text{eff}}$  and  $\log g$  to MIST isochrones (Dotter 2016; Choi et al. 2016). Z23 find a similar  $R_{\star}$  but a higher  $M_{\star} = 0.73 \pm 0.05 M_{\odot}$  using  $\log g$  and  $R_{\star}$  from their SED fit. The infrared mass-luminosity-metallicity derived by Mann et al. (2019) predicts  $M_{\star} = 0.63 \pm 0.02 M_{\odot}$ . Given the unknown nature of the unseen companion, potential for a low-luminosity accretion disk, and likely contamination from the K dwarf chromosphere, we adopt  $M_{\star} = 0.65 \pm 0.05 M_{\odot}$  and  $R_{\star} = 0.65 \pm 0.05 R_{\odot}$  to span all estimates.

The timescale for circularizing and synchronizing the orbit is only  $\approx 10^5$  yr (Zahn 1977) and the low eccentricity ( $e = 0.002 \pm 0.002$ ) reported by Z23 agrees with a tidally-locked binary. Tidal synchronization allows

<sup>3</sup>  $\phi \equiv 0$  corresponds to the visible star in superior conjunction.

<sup>4</sup> We inflate their uncertainties by the average model ‘spread’ reported in Table 6 of Vines & Jenkins (2022):  $\delta T_{\text{eff}} = 3\%$ ,  $\delta \log g = 0.1$  dex,  $\delta R_{\star} = 8\%$ , and  $\delta[\text{Fe}/\text{H}] = 0.2$  dex.

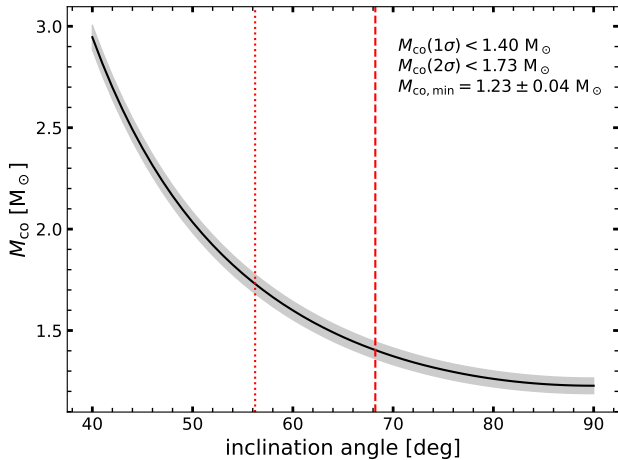


**Figure 2.** We derive  $\sin i = 1.03 \pm 0.10$  from the measured  $v_{\text{rot}} \sin i$  and  $R_*$ .  $i > 90$  deg is unphysical so we report  $1\sigma$  and  $2\sigma$  bounds on  $M_{\text{co}}$  in conjunction with the lower limit required by  $i \equiv 90$  deg.

a direct mass estimate for the unseen companion because  $v_{\text{rot}} = 2\pi R_*/P$  and  $v_{\text{rot}} \sin i = 70.3 \pm 3.9 \text{ km s}^{-1}$  (Table 1). We solve for the inclination angle and find  $\sin i = 1.03 \pm 0.10$ . This implies  $i > 90$  deg which is not physically reasonable, either due to an underestimated  $R_*$  or an overestimated  $v_{\text{rot}} \sin i$ . Z23 find no eclipses in the TESS light curve of J2354, requiring  $i < 90^\circ$ , but the small radii of massive WDs ( $R_{\text{WD}} \lesssim 0.01 R_*$ ) means this constraint is very weak (cf. Fig. 11 in Rowan et al. 2024b). We report  $1\sigma$  and  $2\sigma$  limits on  $M_{\text{co}}$  in Fig. 2 alongside the minimum  $M_{\text{co}}$  assuming  $i \equiv 90^\circ$ . We adopt  $M_{\text{co}} = 1.30^{+0.10}_{-0.05} M_\odot$  for the analysis in §4 which is marginally below the lower estimate quoted by Z23 but consistent within uncertainties. The corresponding orbital separation is  $a = 3.3 \pm 0.1 R_\odot$ .

### 3.2. Individual Abundances

We use Korg’s `fit_spectrum` functionality to measure elemental abundances for J2354. To identify features strong enough to measure elemental abundances, we used Korg’s `prune_linelist` function (with the threshold ratio in line-center absorption to continuum absorption set to 1.0). We then visually inspected the observed and synthetic spectra to narrow down the list of measurable elements. We first fit the whole spectrum with the initial stellar parameters held fixed to initialize a fiducial value for all elements. Then, each feature was fit within a  $10 \text{ \AA}$  window while holding the other abundances fixed. The average abundance and error on the mean for each element are listed in Table 2. Features were excluded from this calculation if they had statistical error greater than one, if they were nondetections (defined as a best-fit  $[X/H] < -3$ ) or (for elements

Element	$[X/H]$ (dex)	$\sigma_{\text{obs}}$	$\sigma_{\text{tot}}$
Na	-0.28	0.20	0.23
Ca	-0.37	0.02	0.10
Sc	-0.60	0.19	0.22
Ti	-0.44	0.06	0.12
V	-0.38	0.08	0.13
Cr	-0.39	0.05	0.11
Mn	-0.66	0.04	0.11
Fe	-0.43	0.02	0.10
Ni	-0.23	0.14	0.17

**Table 2.** Adopted abundance and uncertainties for each element measured from the high-resolution PEPSI spectra. A systematic uncertainty of 0.1 dex is assumed for each. Abundances are given relative to Solar (Asplund et al. 2021).

with more than 20 features) if they were in the region of the sodium D lines. Elements with fewer than three remaining features (Mg and Ba) were excluded. For all elements, the line-to-line scatter is larger than the statistical uncertainty in the per-line abundance. We adopt the standard deviation of the line-to-line estimates as the measurement error, which we add in quadrature to a systematic uncertainty of 0.1 dex for each element. Table 2 lists the abundances and uncertainties for each element, and Appendix A contains further details.

Fig. 3 compares the abundances of J2354 to stars within 100 pc of it based upon the photogeometric distances of Bailer-Jones (2023) that have abundances from the GALactic Archaeology with HERMES (GALAH; Buder et al. 2021) survey.<sup>5</sup> We also show abundances for systems with confirmed or high-confidence compact object companions to search for unique elemental signatures or trends including WDs (Kong et al. 2018a,b), NSs (González Hernández et al. 2005; Hinkle et al. 2006, 2019, 2020; Suárez-Andrés et al. 2015; Shahbaz et al. 2022; El-Badry et al. 2024a) and BHs (Israelian et al. 1999; González Hernández et al. 2004, 2006, 2008, 2011; Sadakane et al. 2006; El-Badry et al. 2023a,b; Gaia Collaboration et al. 2024). Evolved stars ( $\log g < 3.0$  dex) are highlighted because they may experience different mixing and dilution properties than dwarfs. Interestingly, systems that experienced a core-collapse supernova often show evidence for pollution traced by enhanced  $\alpha$  or intermediate-mass elements (IMEs). We note that Fig. 3 obscures the dependence on orbital separation.

<sup>5</sup> Using abundances from the APOGEE experiment (Abdurro’uf et al. 2022) instead of GALAH does not meaningfully change our conclusions.

## 4. IMPLICATIONS FOR THE UNSEEN COMPANION

### 4.1. Neutron Star Scenarios

For a spherical explosion, the amount of polluting material deposited onto the companion’s surface can be estimated assuming it is proportional to the solid angle subtended by the companion,

$$\Delta m_{\text{cap}} = f_{\text{cap}} \times \Delta M \times (\pi R_{\star}/2\pi a_0)^2 \quad (1)$$

where  $\Delta m_{\text{cap}}$  is the mass of polluting material accreted by the companion,  $\Delta M$  is the supernova (SN) ejecta mass,  $R_{\star}$  is the companion radius,  $a_0$  is the pre-explosion orbital separation, and  $f_{\text{cap}}$  is a scaling factor representing the fraction of incident ejecta that stays bound to the K dwarf such that  $f_{\text{cap}} = 0 - 1$ . Simulations show that these simple estimates are generally reasonable - the lower-mass companion will have some mass ablated from the surface which reduces  $f_{\text{cap}}$  for the outer H-rich ejecta but increases  $f_{\text{cap}}$  for the slower-moving inner ejecta (Liu et al. 2015).

J2354 does not show obvious evidence for pollution in Fig. 3 which disfavors a nearby CC SN. In most systems that host a NS or BH the companion shows evidence for atmospheric pollution traced by above-average abundances of IMEs. Variations in ejecta pollution are likely driven by different orbital distances, especially given that the current orbits are not the pre-SN orbits (e.g., Brandt & Podsiadlowski 1995) and the systems in Fig. 3 have a variety of orbital separations. The explosion energy and ejecta mass of the SN will introduce smaller variations in companion pollution, as will mass- and metallicity-dependent nucleosynthesis (e.g., Heger & Woosley 2010; Limongi & Chieffi 2018).

The current orbit is not equal to the pre-SN orbit due to mass ejection by the explosion and the potential for NS kicks (e.g., Sweeney et al. 2022). Moreover, the expected effects of a SN on a  $\sim 0.65 M_{\odot}$  star orbiting just  $\sim 3.3 R_{\odot}$  away are severe. The impacting ejecta will ablate  $\gtrsim 10\%$  of the K dwarf mass, impart a  $\sim 100 \text{ km s}^{-1}$  kick to the K dwarf, and deposit  $\sim 10^{-3} M_{\odot}$  of material onto the surface (Liu et al. 2015), which is in tension with our abundance analysis. Taking the nucleosynthetic yield of a  $15 M_{\odot}$  progenitor from Sukhbold et al. (2016), the accreted mass estimates as a function of orbital separation from Liu et al. (2015), and  $f_{\text{cap}} = 0.1$ , the ejecta would have contributed  $\sim 10\%$  of the total iron-group elements (Mn, Fe, Ni) by mass and  $\sim 25\%$  of the IMEs (Na, Ca, Sc, Ti). This would require an IME-poor K dwarf prior to the SN, at-odds with known trends of increasing  $\alpha$  elements/IMEs with decreasing  $[\text{Fe}/\text{H}]$  (e.g., Hayden et al. 2015).

These tensions can be mitigated by increasing the pre-SN orbital separation to decrease the pollution and allow a more normal abundance pattern in the K dwarf (cf. Fig. 3) prior to the explosion. However, most binaries will expand their orbit after one component explodes due to mass loss from the system. A natal kick of order or higher than the pre-SN orbital velocity is needed to produce a tighter binary (Brandt & Podsiadlowski 1995; Kalogera 1996). Yet less than a third of systems survive such a randomly-oriented kick and only  $\sim 10\%$  will produce tighter binaries. Thus, there must be a balance between increasing the pre-SN separation to reduce atmospheric pollution of the K dwarf and decreasing the orbital separation to improve the chance of producing the correct post-SN orbit.<sup>6</sup>

These are indirect arguments against the unseen companion being a quiescent NS, especially when considering theoretical uncertainties in massive-star evolution, nucleosynthesis, explosion sphericity, and so on. Yet the circumstantial evidence is accumulating given the delicate balance between reducing atmospheric pollution and requiring a tight post-SN orbit. Moreover, a quiescent NS+MS system at  $\approx 127 \text{ pc}$  is a factor of  $\sim 2$  closer than any quiescent NS+MS system reported by El-Badry et al. (2024b,  $d_{\text{min}} \sim 250 \text{ pc}$ ). This corresponds to 1/8th of the search volume, or an increase in the predicted number of quiescent NSs in binaries by almost an order of magnitude. Given the inconclusive evidence for a NS as the dim companion, we reevaluate this assumption in the next section.

### 4.2. White Dwarf Scenarios

Z23 show that the *Swift* UV colors are incompatible with the blackbody-like emission expected for a WD. Instead, they attribute the UV excess to chromospheric activity from the active K-dwarf, supported by H $\alpha$  emission in the LAMOST spectra (and seen in the SNIFS spectrum). Yet they do not explore the possibility that the UV excess can be explained by a combination of chromospheric activity and WD emission.

Fig. 4 shows the allowed parameter space given the GALEX and *Swift* near-UV detection ( $m_{\text{NUV}} = 20.15 \pm 0.11 \text{ mag}$ ) for a blackbody with temperature  $T_{\text{WD}}$  and radius  $R_{\text{WD}}$ . Similar constraints can be obtained from the non-detection a blue continuum in the SNIFS spectrum (cf. Fig. 1). We use the PHOENIX grid of model atmospheres (Husser et al. 2013) to estimate the small contribution of the K dwarf to the UV flux and find where the combined UV fluxes equal the observed flux,

<sup>6</sup> We ignore the kick imparted onto the companion by the SN (Liu et al. 2015) as it only decreases the viability of a surviving binary.

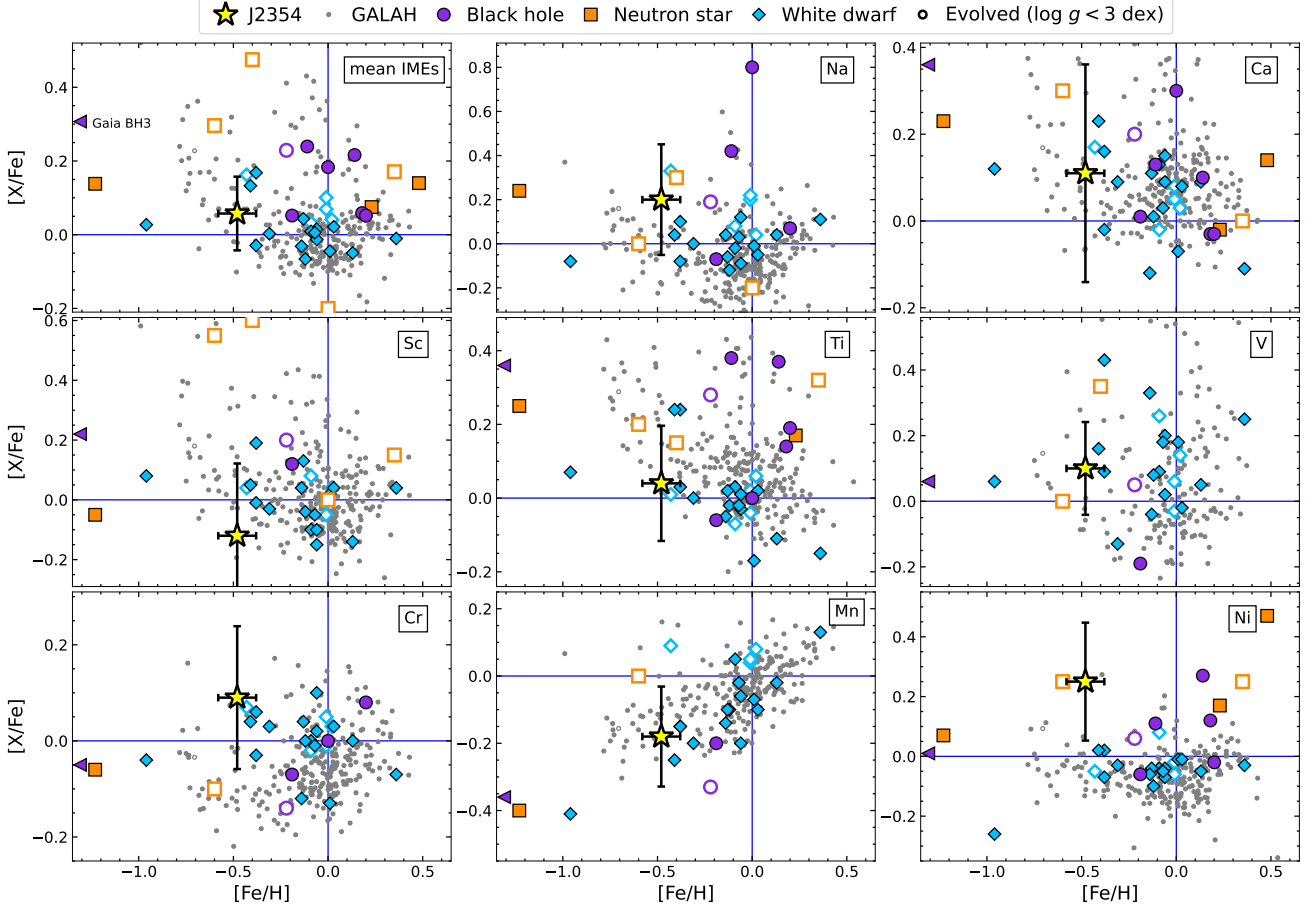


**Figure 3.** The elemental abundances derived for J2354 and the mean IMEs computed from Na, Ca, Ti, and Sc. Stars within 100 pc of J2354 with GALAH DR3 abundances are shown as small gray points. We also show known binary systems hosting black holes (purple), neutron stars (orange) and white dwarfs (blue). Evolved companions ( $\log g < 3$  dex) are shown with open symbols. The purple triangle is the low-metallicity system Gaia BH3 ( $[\text{Fe}/\text{H}] \approx -2.5$  dex) which we have shifted by +1.25 dex for visual clarity. Abundance uncertainties for the comparison sources are typically similar to those we derive for J2354. Thin blue lines mark Solar abundance ratios. References are provided at the end of §3.2.

shown in Fig. 4 as the dark gray region. This is an upper limit on the WD UV flux because there is likely some, and potentially significant, UV flux from the K dwarf chromosphere. Overlaid in Fig. 4 are C/O WD evolutionary tracks from Bédard et al. (2020)<sup>7</sup> showing the increased cooling rate with increasing mass. We show the most conservative cooling tracks, as adopting thinner H layers (Bédard et al. 2020) or O-Ne-Mg cores (Althaus et al. 2022) produces faster cooling or smaller radii, respectively. Including relativistic effects can further shrink the radii of massive WDs by 10 – 20% (Althaus et al. 2022, 2023).<sup>8</sup>

Thus, a massive WD can certainly be hidden by the K dwarf in J2354. As noted by Z23, J2354 would be one of the most massive WDs in a nearby close bi-

nary. J2354 is strikingly similar to the systems identified by Rowan et al. (2024b) with  $\sim 1 M_{\odot}$  WDs orbiting chromospherically-active (spotted) K dwarfs in  $\sim 0.5$ -day orbits. J2354 is also similar to LAMOST J1123 (Yi et al. 2022) which is a claimed quiescent NS + M dwarf binary in a 0.28-d orbit. While K/M dwarfs are common secondaries in canonical post-CE binaries ( $M_{\star} \lesssim 0.8 M_{\odot}$ , Rebassa-Mansergas et al. 2012; Parsons et al. 2016), the cool and massive WDs in J2354 and these similar systems set them apart.

This system also represents an intriguing mass-loss problem. The progenitor ZAMS mass of a  $\sim 1.3 M_{\odot}$  WD is  $M_{\text{ZAMS}} \sim 6 - 8 M_{\odot}$  (e.g., El-Badry et al. 2018; Cunningham et al. 2024). This system would have an initial mass ratio  $q = M_{\text{WD progenitor}}/M_{\text{K dwarf}} \sim 10$  and must have lost  $6 - 1.3 \approx 4.7 M_{\odot}$  of material during post-MS evolution. Yet the Eddington accretion limit of the K dwarf is  $\sim 10^{-8} M_{\odot}/\text{yr}$  so even for a 10-million-year RG phase, the K dwarf accretes  $\lesssim 0.01 M_{\odot}$ . Simula-

<sup>7</sup> <https://www.astro.umontreal.ca/~bergeron/CoolingModels/>

<sup>8</sup> <http://evolgroup.fcaglp.unlp.edu.ar/TRACKS/UMall.html>

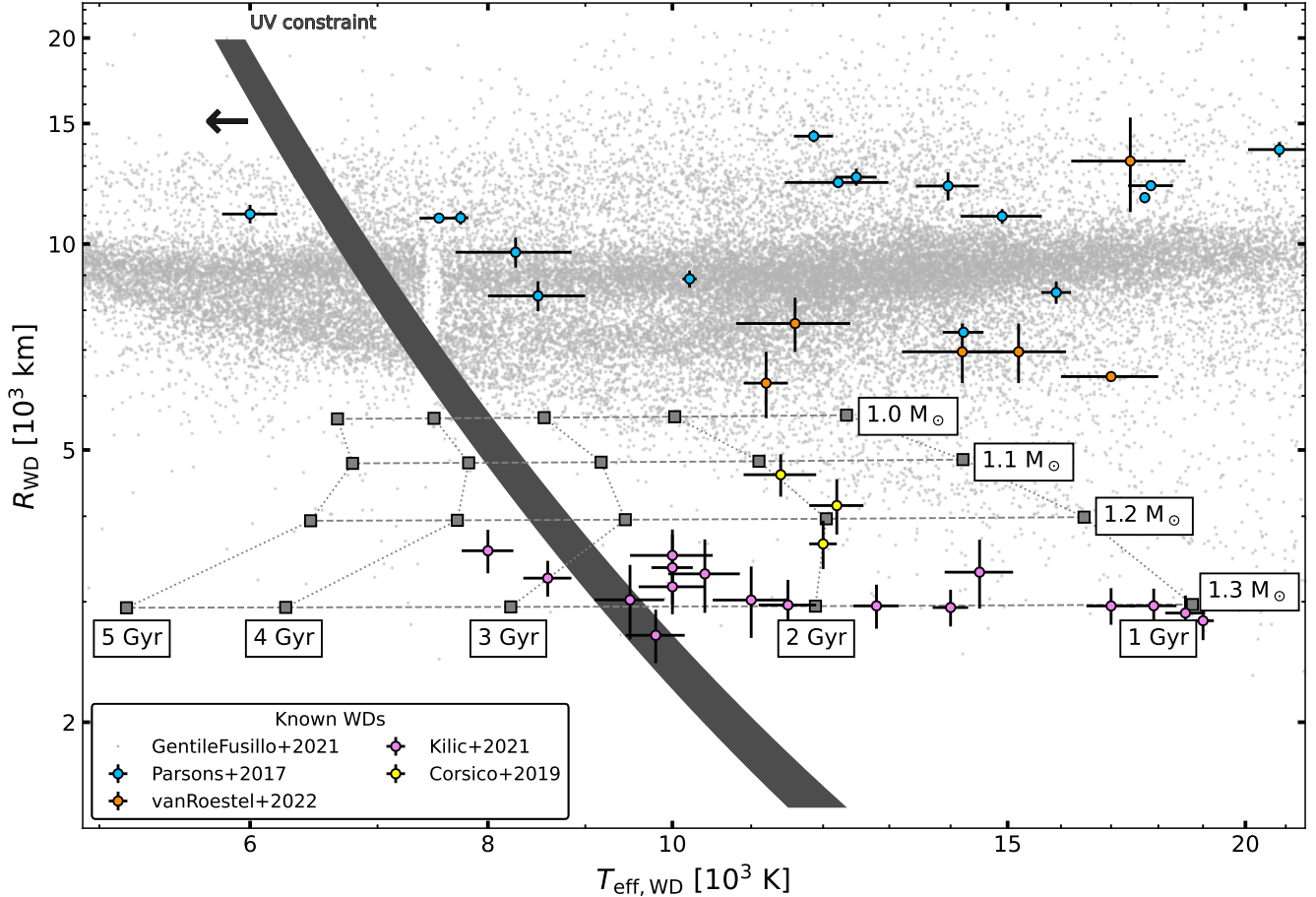


**Figure 4.**  $T_{\text{eff}}$  versus radius for a putative WD companion. The dark-gray region + arrow shows the constraint from the averaged GALEX NUV and *Swift* UVM2 photometry. The combined UV flux from the WD + K dwarf chromosphere must equal this constraint. For comparison, we show known WDs (bold points, Parsons et al. 2017; Córscico et al. 2019; Kilic et al. 2021; van Roestel et al. 2022) and WD candidates from Gaia EDR3 (small gray points, Gentile Fusillo et al. 2021). Overlaid are conservative cooling sequences for massive C/O WDs (bold gray squares) computed by Bédard et al. (2020) showing a  $\sim 1.3 M_{\odot}$  WD with a cooling age of  $\gtrsim 3$  Gyr is allowed. Models adopting O+Ne+Mg cores or thinner H envelopes cool faster, and models including the effects of phase separations or general relativity have even smaller radii (Camisassa et al. 2019, 2022; Althaus et al. 2022, 2023).

tions generally predict limited accretion during CE evolution but it may depend on the specifics of each system (e.g., MacLeod & Ramirez-Ruiz 2015; Chamandy et al. 2018). Higher progenitor masses increases the envelope mass and shortens the RG phase, whereas allowing the K dwarf to accrete significant amounts of material further increases the original mass ratio.

The WD is massive enough for the system to likely experience two CE phases. The envelope is stripped from the more massive companion during the first CE phase, but stars above  $M_{\text{ZAMS}} \sim 2.5 M_{\odot}$  will also undergo He-shell burning. This causes the envelope to expand again to  $\sim 100 R_{\odot}$  (Woosley 2019; Zhang et al. 2024) producing a 2nd CE phase (i.e., ‘Case BB’ mass transfer). This system will almost certainly experience another phase of

mass-transfer in the (distant) future when the K dwarf evolves off of the MS resulting in stable mass-transfer and the formation of a CV.

J2354 and similar short-period high- $q$  binaries (e.g., Rowan et al. 2024b) represent a unique pathway for thermonuclear (Type Ia) supernovae in old stellar populations. The massive WD could accrete matter rapidly enough to ignite C in the core (single-degenerate scenario; Whelan & Iben 1973; Nomoto 1982), inspiral and merge with the RG or AGB core then explode (core-degenerate scenario; Ilkov & Soker 2013; Wang et al. 2017), or inspiral but not merge (double-degenerate scenario) to later experience a double detonation (e.g., Livne 1990; Townsley et al. 2019) or merge as a double-WD binary (e.g., Pakmor et al. 2012, 2013). The out-



come will depend sensitively on the future orbital evolution during mass-transfer as a CV (e.g., Neunteufel et al. 2016).

Finally, we note that there is currently no direct evidence for the companion being a WD, similar to the arguments against a NS outlined in §4.1. A spectrum of the UV excess remains the most promising avenue for direct detection (e.g., Hernandez et al. 2022). Chromospheric activity in low-mass stars produces line-dominated UV emission (France et al. 2016) which contrasts with the smooth blackbody-like spectrum expected for a cool WD (e.g., Caron et al. 2023; Wall et al. 2023). *HST* is the only currently-available facility for such a task. Another interesting prospect for future observations is high-resolution spectroscopy covering lighter species such as CNO, especially isotopologues in the near-IR (e.g., Galan et al. 2016, 2017).

## 5. SUMMARY

We presented follow-up spectroscopy of the enigmatic binary J2354 to better understand the K dwarf and its unseen, massive companion. Overall, the spectra reveal a relatively uninspiring field K dwarf ( $M_{\star} = 0.65 \pm 0.05 M_{\odot}$ ,  $R_{\star} = 0.65 \pm 0.05 R_{\odot}$ ,  $[\text{Fe}/\text{H}] = -0.48 \pm 0.10$  dex) with no peculiar abundances. The improved  $v_{\text{rot}} \sin i$  provides new constraints on the mass of the unseen companion of  $M_{\text{co}} \sim 1.3 M_{\odot}$  with a minimum of  $M_{\text{co,min}} = 1.23 \pm 0.04 M_{\odot}$ . It is difficult to reconcile the normal abundance profile of the K dwarf and the current close-in orbit ( $a = 3.3 \pm 0.1 R_{\odot}$ ) with a NS born from a CC SN. Instead, we find a massive WD the more plausible scenario.

Such a system represents a unique view into close binary evolution at high mass ratio ( $q \approx 10$ ) as the WD progenitor would have started with  $M_{\text{ZAMS}} \approx 6 - 8 M_{\odot}$ . The WD is too massive to have a pure He core so the binary likely experienced 2 phases of CE evolution when the massive companion began H-shell and He-shell burning. This system joins a growing list of massive WDs in close binaries with relatively low-mass ( $M_{\star} \lesssim 1 M_{\odot}$ ) companions. Instead of relying on slow AGB winds to remove the stellar envelope, these systems likely ejected

several  $M_{\odot}$  of material in at least one, possibly two, CE phases. Such systems are extremely useful for placing physical constraints on the complicated processes governing CE evolution and outcomes. Yet J2354 exemplifies the difficulty in distinguishing between high-mass WDs and low-mass NSs in close binaries, even for bright nearby systems.

*Facilities:* UH2.2m (SNIFS); LBT (PEPSI)

*Software:* astropy (Astropy Collaboration et al. 2022); numpy (van der Walt et al. 2011; Harris et al. 2020); matplotlib (Hunter 2007); lmfit (Newville et al. 2014); scipy (Virtanen et al. 2020); spectres (Carnall 2017); emcee (Foreman-Mackey et al. 2013); pandas (The pandas development Team 2024)

## ACKNOWLEDGMENTS

We thank Jennifer Johnson, Marc Pinsonneault, Chris Kochanek, Kris Stanek, Dan Huber, Ben Shappee, and Todd Thompson for useful discussions.

The LBT is an international collaboration among institutions in the United States, Italy, and Germany. LBT Corporation partners are: The University of Arizona on behalf of the Arizona Board of Regents; Istituto Nazionale di Astrofisica, Italy; LBT Beteiligungsgesellschaft, Germany, representing the Max-Planck Society, The Leibniz Institute for Astrophysics Potsdam, and Heidelberg University; The Ohio State University, representing OSU, University of Notre Dame, University of Minnesota, and University of Virginia. PEPSI was made possible by funding through the State of Brandenburg (MWFK) and the German Federal Ministry of Education and Research (BMBF) through their Verbundforschung grants 05AL2BA1/3 and 05A08BAC.

## APPENDIX

### A. ADDITIONAL SPECTROSCOPIC AND ABUNDANCE INFORMATION

Table 3 provides exposure-specific information for each of the PEPSI spectra. RVs are measured using a template matching the parameters given in Table 1. Using a template with  $v_{\text{rot}} \sin i = 20 \text{ km s}^{-1}$  finds values consistent within  $1\sigma$ . Fig. 5 shows that the individual PEPSI spectra does not exhibit any evolution in line strengths or widths. Fig. 6

Exposure Start (UTC)	JD-TDB	Phase	$RV_{\text{blue}}$	$RV_{\text{red}}$	$RV_{Z23}$
2022-10-14 02:19:38	2459866.616501445	0.33 – 0.39	$210.4 \pm 6.6$	$204.5 \pm 5.0$	212.9
2022-10-14 03:00:25	2459866.644826776	0.27 – 0.33	$247.4 \pm 6.0$	$243.5 \pm 3.4$	250.6
2022-10-14 03:41:13	2459866.673155239	0.21 – 0.27	$255.6 \pm 5.7$	$250.7 \pm 3.6$	259.8

**Table 3.** Information for the individual PEPSI exposures. RVs are given in  $\text{km s}^{-1}$ . Phases are computed using the Z23 ephemeris. The Barycentric Dynamical Time Julian Date (JD-TDB) corresponds to the middle of each exposure. Radial velocities are measured by cross-correlating the observed spectrum and a synthetic template with the derived spectroscopic parameters reported in Table 1 in *iSpec* (Blanco-Cuaresma et al. 2014).

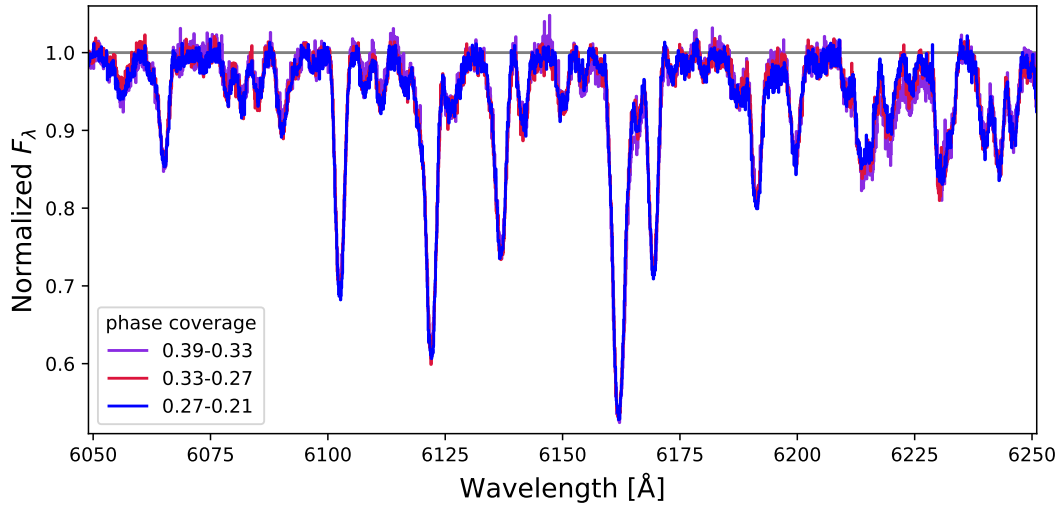


**Figure 5.** Subset of each PEPSI exposure at native resolution showing stable line profiles.

shows the individual abundance measurements for each element and adopted mean given in Table 2. Finally, Table 4 contains the linelist citations for the species measured in the PEPSI spectra.

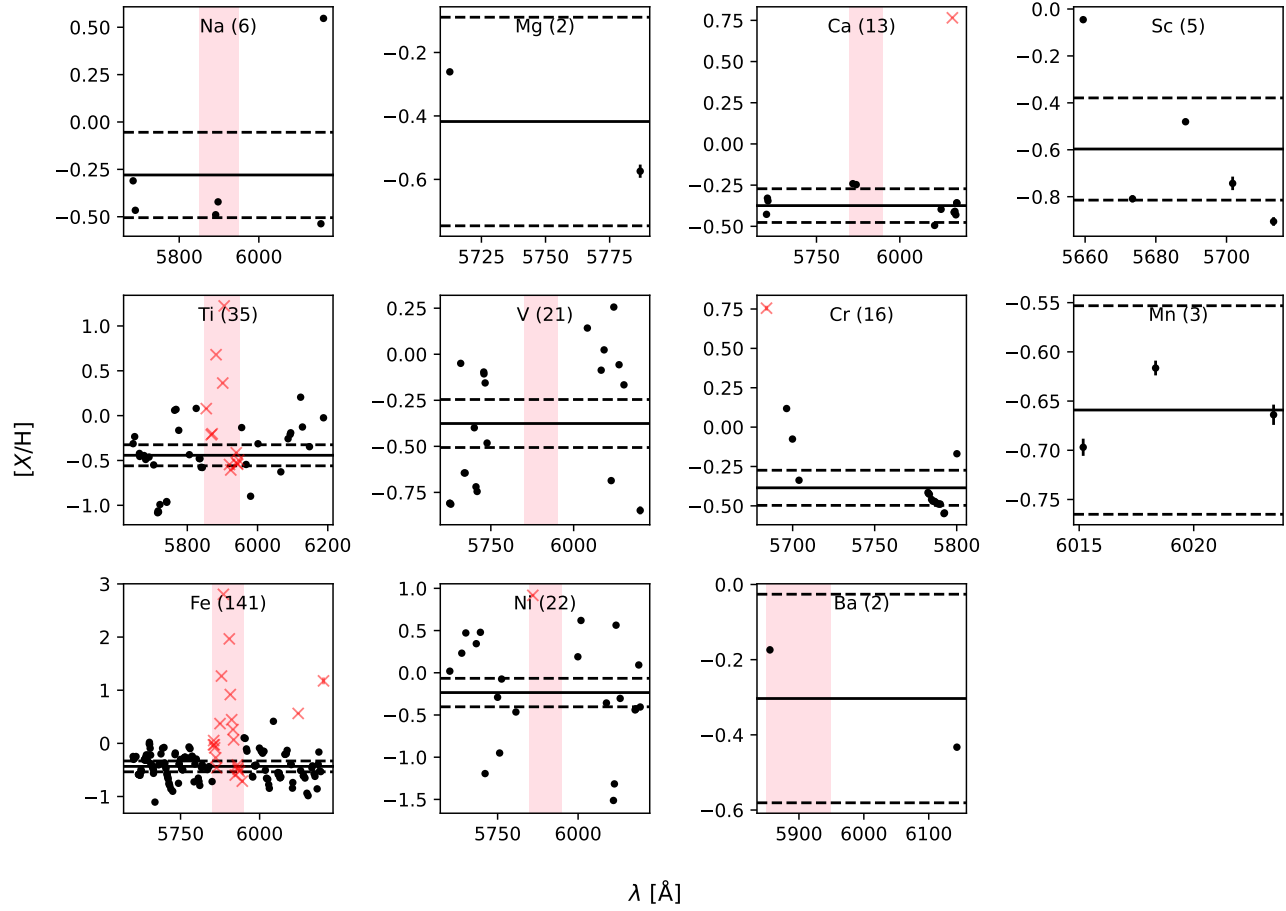


**Figure 6.** Individual abundance measurements for each element. Solid and dashed black lines represent the mean abundance and its uncertainty which are reported in Table 2. Those excluded from abundance estimation are marked with red "x"s. A pink vertical band marks the region of the sodium D lines. Solid and dashed horizontal lines mark the adopted abundance and uncertainties, respectively. Ba and Mg are excluded from our analysis because they only have 2 detected lines.

Element	References
Na	Barklem et al. (2000), Ralchenko et al. (2010), Kurucz & Peytremann (1975), Wiese et al. (1966)
Mg	Kurucz & Peytremann (1975), Barklem et al. (2000), Ralchenko et al. (2010), Lincke & Ziegenbein (1971)
Ca	Kurucz (2007), Smith & Raggett (1981), Smith (1988), Barklem et al. (2000), Smith & O’Neill (1975)
Sc	Kurucz (2009), Barklem et al. (2000), Lawler et al. (2019), Kramida et al. (2022), Lawler & Dakin (1989)
Ti	Barklem et al. (2000), Lawler et al. (2013), Kurucz (2016), Saloman (2012), Wood et al. (2013), Karlsson & Litzén (2000), Nitz et al. (1998), Forsberg (1991)
V	Kurucz (2009), Lawler et al. (2014), Thorne et al. (2011), Barklem et al. (2000), Martin et al. (1988)
Cr	Kurucz (2016), Barklem et al. (2000), Sobek et al. (2007), Kramida et al. (2022), Barklem & Aspelund-Johansson (2005), Lawler et al. (2017), Martin et al. (1988)
Mn	Kurucz (2007), Barklem et al. (2000), Martin et al. (1988), Blackwell-Whitehead et al. (2005), Den Hartog et al. (2011), Sugar & Corliss (1985)
Fe	Kurucz (2014), Barklem et al. (2000), Kurucz (2013), Barklem & Aspelund-Johansson (2005)
Ni	Kurucz (2008); Wood et al. (2014); Litzén et al. (1993); Barklem et al. (2000); Fuhr et al. (1988)
Ba	Corliss & Bozman (1962); Miles & Wiese (1969); Barklem et al. (2000)

**Table 4.** VALD linelist references for the elements measured in §3.2.

## REFERENCES

- Abdurro'uf, Accetta, K., Aerts, C., et al. 2022, *ApJS*, 259, 35, doi: [10.3847/1538-4365/ac4414](https://doi.org/10.3847/1538-4365/ac4414)
- Althaus, L. G., Camisassa, M. E., Torres, S., et al. 2022, *A&A*, 668, A58, doi: [10.1051/0004-6361/202244604](https://doi.org/10.1051/0004-6361/202244604)
- Althaus, L. G., Córscico, A. H., Camisassa, M. E., et al. 2023, *MNRAS*, 523, 4492, doi: [10.1093/mnras/stad1720](https://doi.org/10.1093/mnras/stad1720)
- Asplund, M., Amarsi, A. M., & Grevesse, N. 2021, *A&A*, 653, A141, doi: [10.1051/0004-6361/202140445](https://doi.org/10.1051/0004-6361/202140445)
- Astropy Collaboration, Price-Whelan, A. M., Lim, P. L., et al. 2022, *ApJ*, 935, 167, doi: [10.3847/1538-4357/ac7c74](https://doi.org/10.3847/1538-4357/ac7c74)
- Bailer-Jones, C. A. L. 2023, *AJ*, 166, 269, doi: [10.3847/1538-3881/ad08bb](https://doi.org/10.3847/1538-3881/ad08bb)
- Barklem, P. S., & Aspelund-Johansson, J. 2005, *Astron. and Astrophys.*, 435, 373, doi: [10.1051/0004-6361:20042469](https://doi.org/10.1051/0004-6361:20042469)
- Barklem, P. S., Piskunov, N., & O'Mara, B. J. 2000, *Astron. and Astrophys. Suppl. Ser.*, 142, 467, doi: [10.1051/aas:2000167](https://doi.org/10.1051/aas:2000167)
- Barlow, E. J., Knigge, C., Bird, A. J., et al. 2006, *MNRAS*, 372, 224, doi: [10.1111/j.1365-2966.2006.10836.x](https://doi.org/10.1111/j.1365-2966.2006.10836.x)
- Bédard, A., Bergeron, P., Brassard, P., & Fontaine, G. 2020, *ApJ*, 901, 93, doi: [10.3847/1538-4357/abafbe](https://doi.org/10.3847/1538-4357/abafbe)
- Belloni, D., Zorotovic, M., Schreiber, M. R., et al. 2024, *A&A*, 686, A61, doi: [10.1051/0004-6361/202449235](https://doi.org/10.1051/0004-6361/202449235)
- Blackwell-Whitehead, R. J., Xu, H. L., Pickering, J. C., Nave, G., & Lundberg, H. 2005, *MNRAS*, 361, 1281, doi: [10.1111/j.1365-2966.2005.09264.x](https://doi.org/10.1111/j.1365-2966.2005.09264.x)
- Blanco-Cuaresma, S., Soubiran, C., Heiter, U., & Jofré, P. 2014, *A&A*, 569, A111, doi: [10.1051/0004-6361/201423945](https://doi.org/10.1051/0004-6361/201423945)
- Brandt, N., & Podsiadlowski, P. 1995, *MNRAS*, 274, 461, doi: [10.1093/mnras/274.2.461](https://doi.org/10.1093/mnras/274.2.461)
- Buder, S., Sharma, S., Kos, J., et al. 2021, *MNRAS*, 506, 150, doi: [10.1093/mnras/stab1242](https://doi.org/10.1093/mnras/stab1242)
- Camisassa, M. E., Althaus, L. G., Koester, D., et al. 2022, *MNRAS*, 511, 5198, doi: [10.1093/mnras/stac348](https://doi.org/10.1093/mnras/stac348)
- Camisassa, M. E., Althaus, L. G., Córscico, A. H., et al. 2019, *A&A*, 625, A87, doi: [10.1051/0004-6361/201833822](https://doi.org/10.1051/0004-6361/201833822)
- Carnall, A. C. 2017, arXiv e-prints, arXiv:1705.05165, doi: [10.48550/arXiv.1705.05165](https://doi.org/10.48550/arXiv.1705.05165)
- Caron, A., Bergeron, P., Blouin, S., & Leggett, S. K. 2023, *MNRAS*, 519, 4529, doi: [10.1093/mnras/stac3733](https://doi.org/10.1093/mnras/stac3733)
- Chamandy, L., Frank, A., Blackman, E. G., et al. 2018, *MNRAS*, 480, 1898, doi: [10.1093/mnras/sty1950](https://doi.org/10.1093/mnras/sty1950)
- Choi, J., Dotter, A., Conroy, C., et al. 2016, *ApJ*, 823, 102, doi: [10.3847/0004-637X/823/2/102](https://doi.org/10.3847/0004-637X/823/2/102)
- Corliss, C. H., & Bozman, W. R. 1962, NBS Monograph, Vol. 53, Experimental transition probabilities for spectral lines of seventy elements; derived from the NBS Tables of spectral-line intensities, ed. Corliss, C. H. & Bozman, W. R. (US Government Printing Office)
- Córscico, A. H., De Gerónimo, F. C., Camisassa, M. E., & Althaus, L. G. 2019, *A&A*, 632, A119, doi: [10.1051/0004-6361/201936698](https://doi.org/10.1051/0004-6361/201936698)
- Cummings, J. D., Kalirai, J. S., Tremblay, P. E., Ramirez-Ruiz, E., & Choi, J. 2018, *ApJ*, 866, 21, doi: [10.3847/1538-4357/aadfd6](https://doi.org/10.3847/1538-4357/aadfd6)
- Cunningham, T., Tremblay, P.-E., & W. O'Brien, M. 2024, *MNRAS*, 527, 3602, doi: [10.1093/mnras/stad3275](https://doi.org/10.1093/mnras/stad3275)
- Den Hartog, E. A., Lawler, J. E., Sobek, J. S., Sneden, C., & Cowan, J. J. 2011, *ApJS*, 194, 35, doi: [10.1088/0067-0049/194/2/35](https://doi.org/10.1088/0067-0049/194/2/35)
- Dharmawardena, T. E., Bailer-Jones, C. A. L., Fouesneau, M., et al. 2024, *MNRAS*, doi: [10.1093/mnras/stae1474](https://doi.org/10.1093/mnras/stae1474)
- Dotter, A. 2016, *ApJS*, 222, 8, doi: [10.3847/0067-0049/222/1/8](https://doi.org/10.3847/0067-0049/222/1/8)
- Drake, A. J., Gänsicke, B. T., Djorgovski, S. G., et al. 2014, *MNRAS*, 441, 1186, doi: [10.1093/mnras/stu639](https://doi.org/10.1093/mnras/stu639)
- El-Badry, K., Rix, H.-W., & Weisz, D. R. 2018, *ApJL*, 860, L17, doi: [10.3847/2041-8213/aaca9c](https://doi.org/10.3847/2041-8213/aaca9c)
- El-Badry, K., Rix, H.-W., Quataert, E., et al. 2023a, *MNRAS*, 518, 1057, doi: [10.1093/mnras/stac3140](https://doi.org/10.1093/mnras/stac3140)
- El-Badry, K., Rix, H.-W., Cendes, Y., et al. 2023b, *MNRAS*, 521, 4323, doi: [10.1093/mnras/stad799](https://doi.org/10.1093/mnras/stad799)
- El-Badry, K., Simon, J. D., Reggiani, H., et al. 2024a, *The Open Journal of Astrophysics*, 7, 27, doi: [10.33232/001c.116675](https://doi.org/10.33232/001c.116675)
- . 2024b, arXiv e-prints, arXiv:2402.06722, doi: [10.48550/arXiv.2402.06722](https://doi.org/10.48550/arXiv.2402.06722)
- Fantin, N. J., Côté, P., McConnachie, A. W., et al. 2019, *ApJ*, 887, 148, doi: [10.3847/1538-4357/ab5521](https://doi.org/10.3847/1538-4357/ab5521)
- Foreman-Mackey, D., Hogg, D. W., Lang, D., & Goodman, J. 2013, *PASP*, 125, 306, doi: [10.1086/670067](https://doi.org/10.1086/670067)
- Forsberg, P. 1991, *PhyS*, 44, 446, doi: [10.1088/0031-8949/44/5/008](https://doi.org/10.1088/0031-8949/44/5/008)
- France, K., Loyd, R. O. P., Youngblood, A., et al. 2016, *ApJ*, 820, 89, doi: [10.3847/0004-637X/820/2/89](https://doi.org/10.3847/0004-637X/820/2/89)
- Fuhr, J. R., Martin, G. A., & Wiese, W. L. 1988, *Journal of Physical and Chemical Reference Data*, Volume 17, Suppl. 4. New York: American Institute of Physics (AIP) and American Chemical Society, 1988, 17
- Gaia Collaboration, Panuzzo, P., Mazeh, T., et al. 2024, *A&A*, 686, L2, doi: [10.1051/0004-6361/202449763](https://doi.org/10.1051/0004-6361/202449763)
- Gałań, C., Mikołajewska, J., Hinkle, K. H., & Joyce, R. R. 2016, *MNRAS*, 455, 1282, doi: [10.1093/mnras/stv2365](https://doi.org/10.1093/mnras/stv2365)

- . 2017, MNRAS, 466, 2194, doi: [10.1093/mnras/stw3266](https://doi.org/10.1093/mnras/stw3266)
- Garbutt, J. A., Parsons, S. G., Toloza, O., et al. 2024, MNRAS, 529, 4840, doi: [10.1093/mnras/stae807](https://doi.org/10.1093/mnras/stae807)
- Gentile Fusillo, N. P., Tremblay, P. E., Cukanovaite, E., et al. 2021, MNRAS, 508, 3877, doi: [10.1093/mnras/stab2672](https://doi.org/10.1093/mnras/stab2672)
- González Hernández, J. I., Casares, J., Rebolo, R., et al. 2011, ApJ, 738, 95, doi: [10.1088/0004-637X/738/1/95](https://doi.org/10.1088/0004-637X/738/1/95)
- González Hernández, J. I., Rebolo, R., Israelian, G., et al. 2005, ApJ, 630, 495, doi: [10.1086/430755](https://doi.org/10.1086/430755)
- . 2004, ApJ, 609, 988, doi: [10.1086/421102](https://doi.org/10.1086/421102)
- . 2008, ApJ, 679, 732, doi: [10.1086/586888](https://doi.org/10.1086/586888)
- . 2006, ApJL, 644, L49, doi: [10.1086/505391](https://doi.org/10.1086/505391)
- Gray, R. O., McGahee, C. E., Griffin, R. E. M., & Corbally, C. J. 2011, AJ, 141, 160, doi: [10.1088/0004-6256/141/5/160](https://doi.org/10.1088/0004-6256/141/5/160)
- Green, G. M., Schlafly, E., Zucker, C., Speagle, J. S., & Finkbeiner, D. 2019, ApJ, 887, 93, doi: [10.3847/1538-4357/ab5362](https://doi.org/10.3847/1538-4357/ab5362)
- Harris, C. R., Millman, K. J., van der Walt, S. J., et al. 2020, Nature, 585, 357, doi: [10.1038/s41586-020-2649-2](https://doi.org/10.1038/s41586-020-2649-2)
- Hayden, M. R., Bovy, J., Holtzman, J. A., et al. 2015, ApJ, 808, 132, doi: [10.1088/0004-637X/808/2/132](https://doi.org/10.1088/0004-637X/808/2/132)
- Hegedűs, V., Mészáros, S., Jofré, P., et al. 2023, A&A, 670, A107, doi: [10.1051/0004-6361/202244813](https://doi.org/10.1051/0004-6361/202244813)
- Heger, A., & Woosley, S. E. 2010, ApJ, 724, 341, doi: [10.1088/0004-637X/724/1/341](https://doi.org/10.1088/0004-637X/724/1/341)
- Hernandez, M. S., Schreiber, M. R., Parsons, S. G., et al. 2022, MNRAS, 517, 2867, doi: [10.1093/mnras/stac2837](https://doi.org/10.1093/mnras/stac2837)
- Hinkle, K. H., Fekel, F. C., Joyce, R. R., et al. 2019, ApJ, 872, 43, doi: [10.3847/1538-4357/aafba5](https://doi.org/10.3847/1538-4357/aafba5)
- . 2006, ApJ, 641, 479, doi: [10.1086/500350](https://doi.org/10.1086/500350)
- Hinkle, K. H., Lebzelter, T., Fekel, F. C., et al. 2020, ApJ, 904, 143, doi: [10.3847/1538-4357/abbe01](https://doi.org/10.3847/1538-4357/abbe01)
- Hunter, J. D. 2007, Computing in Science and Engineering, 9, 90, doi: [10.1109/MCSE.2007.55](https://doi.org/10.1109/MCSE.2007.55)
- Husser, T. O., Wende-von Berg, S., Dreizler, S., et al. 2013, A&A, 553, A6, doi: [10.1051/0004-6361/201219058](https://doi.org/10.1051/0004-6361/201219058)
- Ilkov, M., & Soker, N. 2013, MNRAS, 428, 579, doi: [10.1093/mnras/sts053](https://doi.org/10.1093/mnras/sts053)
- Israelian, G., Rebolo, R., Basri, G., Casares, J., & Martín, E. L. 1999, Nature, 401, 142, doi: [10.1038/43625](https://doi.org/10.1038/43625)
- Ivanova, N. 2011, ApJ, 730, 76, doi: [10.1088/0004-637X/730/2/76](https://doi.org/10.1088/0004-637X/730/2/76)
- Jayasinghe, T., Rowan, D. M., Thompson, T. A., Kochanek, C. S., & Stanek, K. Z. 2023, MNRAS, 521, 5927, doi: [10.1093/mnras/stad909](https://doi.org/10.1093/mnras/stad909)
- Jenkins, S., Vanderburg, A., Bieryla, A., et al. 2024, MNRAS, doi: [10.1093/mnras/stae1506](https://doi.org/10.1093/mnras/stae1506)
- Jofré, P., Heiter, U., & Soubiran, C. 2019, ARA&A, 57, 571, doi: [10.1146/annurev-astro-091918-104509](https://doi.org/10.1146/annurev-astro-091918-104509)
- Kalogera, V. 1996, ApJ, 471, 352, doi: [10.1086/177974](https://doi.org/10.1086/177974)
- Karlsson, H., & Litzén, U. 2000, Journal of Physics B Atomic Molecular Physics, 33, 2929, doi: [10.1088/0953-4075/33/15/309](https://doi.org/10.1088/0953-4075/33/15/309)
- Kesseli, A. Y., West, A. A., Veyette, M., et al. 2017, ApJS, 230, 16, doi: [10.3847/1538-4365/aa656d](https://doi.org/10.3847/1538-4365/aa656d)
- Kilic, M., Bergeron, P., Blouin, S., & Bédard, A. 2021, MNRAS, 503, 5397, doi: [10.1093/mnras/stab767](https://doi.org/10.1093/mnras/stab767)
- Kong, X. M., Bharat Kumar, Y., Zhao, G., et al. 2018a, MNRAS, 474, 2129, doi: [10.1093/mnras/stx2809](https://doi.org/10.1093/mnras/stx2809)
- Kong, X. M., Zhao, G., Zhao, J. K., et al. 2018b, MNRAS, 476, 724, doi: [10.1093/mnras/sty280](https://doi.org/10.1093/mnras/sty280)
- Kosakowski, A., Kilic, M., Brown, W. R., & Gianninas, A. 2020, ApJ, 894, 53, doi: [10.3847/1538-4357/ab8300](https://doi.org/10.3847/1538-4357/ab8300)
- Kramida, A., Ralchenko, Y., Reader, J., & NIST ASD Team. 2022, NIST Atomic Spectra Database (ver. 5.10), [Online]., National Institute of Standards and Technology, Gaithersburg, MD.
- Kurucz, R. L. 2007, Robert L. Kurucz on-line database of observed and predicted atomic transitions
- . 2008, Robert L. Kurucz on-line database of observed and predicted atomic transitions
- . 2009, Robert L. Kurucz on-line database of observed and predicted atomic transitions
- . 2013, Robert L. Kurucz on-line database of observed and predicted atomic transitions
- . 2014, Robert L. Kurucz on-line database of observed and predicted atomic transitions
- . 2016, Robert L. Kurucz on-line database of observed and predicted atomic transitions
- Kurucz, R. L., & Peytremann, E. 1975, SAO Special Report, 362, 1
- Lantz, B., Aldering, G., Antilogus, P., et al. 2004, in Society of Photo-Optical Instrumentation Engineers (SPIE) Conference Series, Vol. 5249, Optical Design and Engineering, ed. L. Mazuray, P. J. Rogers, & R. Wartmann, 146–155, doi: [10.1117/12.512493](https://doi.org/10.1117/12.512493)
- Lawler, J. E., & Dakin, J. T. 1989, Journal of the Optical Society of America B Optical Physics, 6, 1457, doi: [10.1364/JOSAB.6.001457](https://doi.org/10.1364/JOSAB.6.001457)
- Lawler, J. E., Guzman, A., Wood, M. P., Sneden, C., & Cowan, J. J. 2013, ApJS, 205, 11, doi: [10.1088/0067-0049/205/2/11](https://doi.org/10.1088/0067-0049/205/2/11)
- Lawler, J. E., Hala, Sneden, C., et al. 2019, ApJS, 241, 21, doi: [10.3847/1538-4365/ab08ef](https://doi.org/10.3847/1538-4365/ab08ef)
- Lawler, J. E., Sneden, C., Nave, G., et al. 2017, ApJS, 228, 10, doi: [10.3847/1538-4365/228/1/10](https://doi.org/10.3847/1538-4365/228/1/10)

- Lawler, J. E., Wood, M. P., Den Hartog, E. A., et al. 2014, *ApJS*, 215, 20, doi: [10.1088/0067-0049/215/2/20](https://doi.org/10.1088/0067-0049/215/2/20)
- Limongi, M., & Chieffi, A. 2018, *ApJS*, 237, 13, doi: [10.3847/1538-4365/aac24](https://doi.org/10.3847/1538-4365/aac24)
- Lincke, R., & Ziegenbein, B. 1971, *Zeitschrift für Physik*, 241, 369, doi: [10.1007/BF01395433](https://doi.org/10.1007/BF01395433)
- Litzèn, U., Brault, J. W., & Thorne, A. P. 1993, *PhyS*, 47, 628, doi: [10.1088/0031-8949/47/5/004](https://doi.org/10.1088/0031-8949/47/5/004)
- Liu, H.-B., Gu, W.-M., Zhang, Z.-X., et al. 2024, arXiv e-prints, arXiv:2405.09825, doi: [10.48550/arXiv.2405.09825](https://doi.org/10.48550/arXiv.2405.09825)
- Liu, Z.-W., Tauris, T. M., Röpke, F. K., et al. 2015, *A&A*, 584, A11, doi: [10.1051/0004-6361/201526757](https://doi.org/10.1051/0004-6361/201526757)
- Livne, E. 1990, *ApJL*, 354, L53, doi: [10.1086/185721](https://doi.org/10.1086/185721)
- MacLeod, M., & Ramirez-Ruiz, E. 2015, *ApJ*, 803, 41, doi: [10.1088/0004-637X/803/1/41](https://doi.org/10.1088/0004-637X/803/1/41)
- Manchester, R. N., Hobbs, G. B., Teoh, A., & Hobbs, M. 2005, *AJ*, 129, 1993, doi: [10.1086/428488](https://doi.org/10.1086/428488)
- Mann, A. W., Dupuy, T., Kraus, A. L., et al. 2019, *ApJ*, 871, 63, doi: [10.3847/1538-4357/aaf3bc](https://doi.org/10.3847/1538-4357/aaf3bc)
- Marchant, P., Pappas, K. M. W., Gallegos-Garcia, M., et al. 2021, *A&A*, 650, A107, doi: [10.1051/0004-6361/202039992](https://doi.org/10.1051/0004-6361/202039992)
- Martin, G., Fuhr, J., & Wiese, W. 1988, *J. Phys. Chem. Ref. Data Suppl.*, 17
- Miles, B. M., & Wiese, W. L. 1969, *Atomic Data*, 1, 1, doi: [10.1016/S0092-640X\(69\)80019-7](https://doi.org/10.1016/S0092-640X(69)80019-7)
- Moe, M., & Di Stefano, R. 2017, *ApJS*, 230, 15, doi: [10.3847/1538-4365/aa6fb6](https://doi.org/10.3847/1538-4365/aa6fb6)
- Neunteufel, P., Yoon, S. C., & Langer, N. 2016, *A&A*, 589, A43, doi: [10.1051/0004-6361/201527845](https://doi.org/10.1051/0004-6361/201527845)
- Newville, M., Stensitzki, T., Allen, D. B., & Ingargiola, A. 2014, *LMFIT: Non-Linear Least-Square Minimization and Curve-Fitting for Python*, 0.8.0, Zenodo, doi: [10.5281/zenodo.11813](https://doi.org/10.5281/zenodo.11813)
- Nitz, D. E., Wickliffe, M. E., & Lawler, J. E. 1998, *Astrophys. J. Suppl. Ser.*, 117, 313, doi: [10.1086/313112](https://doi.org/10.1086/313112)
- Nomoto, K. 1982, *ApJ*, 253, 798, doi: [10.1086/159682](https://doi.org/10.1086/159682)
- Özel, F., Psaltis, D., Narayan, R., & Santos Villarreal, A. 2012, *ApJ*, 757, 55, doi: [10.1088/0004-637X/757/1/55](https://doi.org/10.1088/0004-637X/757/1/55)
- Pakmor, R., Kromer, M., Taubenberger, S., et al. 2012, *ApJL*, 747, L10, doi: [10.1088/2041-8205/747/1/L10](https://doi.org/10.1088/2041-8205/747/1/L10)
- Pakmor, R., Kromer, M., Taubenberger, S., & Springel, V. 2013, *ApJL*, 770, L8, doi: [10.1088/2041-8205/770/1/L8](https://doi.org/10.1088/2041-8205/770/1/L8)
- Parsons, S. G., Rebassa-Mansergas, A., Schreiber, M. R., et al. 2016, *MNRAS*, 463, 2125, doi: [10.1093/mnras/stw2143](https://doi.org/10.1093/mnras/stw2143)
- Parsons, S. G., Gänsicke, B. T., Marsh, T. R., et al. 2017, *MNRAS*, 470, 4473, doi: [10.1093/mnras/stx1522](https://doi.org/10.1093/mnras/stx1522)
- Piskunov, N. E., Kupka, F., Ryabchikova, T. A., Weiss, W. W., & Jeffery, C. S. 1995, *A&AS*, 112, 525
- Postnov, K. A., & Yungelson, L. R. 2014, *Living Reviews in Relativity*, 17, 3, doi: [10.12942/lrr-2014-3](https://doi.org/10.12942/lrr-2014-3)
- Ralchenko, Y., Kramida, A., Reader, J., & NIST ASD Team. 2010, *NIST Atomic Spectra Database (ver. 4.0.0)*, [Online]., National Institute of Standards and Technology, Gaithersburg, MD.
- Rebassa-Mansergas, A., Nebot Gómez-Morán, A., Schreiber, M. R., et al. 2012, *MNRAS*, 419, 806, doi: [10.1111/j.1365-2966.2011.19923.x](https://doi.org/10.1111/j.1365-2966.2011.19923.x)
- Rebassa-Mansergas, A., Solano, E., Jiménez-Esteban, F. M., et al. 2021, *MNRAS*, 506, 5201, doi: [10.1093/mnras/stab2039](https://doi.org/10.1093/mnras/stab2039)
- Ritter, H., & Kolb, U. 2003, *A&A*, 404, 301, doi: [10.1051/0004-6361:20030330](https://doi.org/10.1051/0004-6361:20030330)
- Röpke, F. K., & De Marco, O. 2023, *Living Reviews in Computational Astrophysics*, 9, 2, doi: [10.1007/s41115-023-00017-x](https://doi.org/10.1007/s41115-023-00017-x)
- Roulston, B. R., Green, P. J., & Kesseli, A. Y. 2020, *ApJS*, 249, 34, doi: [10.3847/1538-4365/aba1e7](https://doi.org/10.3847/1538-4365/aba1e7)
- Rowan, D. M., Thompson, T. A., Jayasinghe, T., Kochanek, C. S., & Stanek, K. Z. 2024a, *The Open Journal of Astrophysics*, 7, 24, doi: [10.33232/001c.116170](https://doi.org/10.33232/001c.116170)
- Rowan, D. M., Jayasinghe, T., Tucker, M. A., et al. 2024b, *MNRAS*, 529, 587, doi: [10.1093/mnras/stae517](https://doi.org/10.1093/mnras/stae517)
- Ryabchikova, T., Piskunov, N., Kurucz, R. L., et al. 2015, *PhyS*, 90, 054005, doi: [10.1088/0031-8949/90/5/054005](https://doi.org/10.1088/0031-8949/90/5/054005)
- Sadakane, K., Arai, A., Aoki, W., et al. 2006, *PASJ*, 58, 595, doi: [10.1093/pasj/58.3.595](https://doi.org/10.1093/pasj/58.3.595)
- Saloman, E. B. 2012, *Journal of Physical and Chemical Reference Data*, 41, 013101, doi: [10.1063/1.3656882](https://doi.org/10.1063/1.3656882)
- Scherbak, P., & Fuller, J. 2023, *MNRAS*, 518, 3966, doi: [10.1093/mnras/stac3313](https://doi.org/10.1093/mnras/stac3313)
- Schwöpe, A., Kurpas, J., Baecke, P., et al. 2024, *A&A*, 686, A110, doi: [10.1051/0004-6361/202348426](https://doi.org/10.1051/0004-6361/202348426)
- Shahaf, S., Hallakoun, N., Mazeh, T., et al. 2024, *MNRAS*, 529, 3729, doi: [10.1093/mnras/stae773](https://doi.org/10.1093/mnras/stae773)
- Shahbaz, T., González-Hernández, J. I., Breton, R. P., et al. 2022, *MNRAS*, 513, 71, doi: [10.1093/mnras/stac492](https://doi.org/10.1093/mnras/stac492)
- Smith, G. 1988, *Journal of Physics B Atomic Molecular Physics*, 21, 2827, doi: [10.1088/0953-4075/21/16/008](https://doi.org/10.1088/0953-4075/21/16/008)
- Smith, G., & O'Neill, J. A. 1975, *Astron. and Astrophys.*, 38, 1
- Smith, G., & Raggett, D. S. J. 1981, *Journal of Physics B Atomic Molecular Physics*, 14, 4015, doi: [10.1088/0022-3700/14/21/016](https://doi.org/10.1088/0022-3700/14/21/016)
- Sobeck, J. S., Lawler, J. E., & Sneden, C. 2007, *Astrophys. J.*, 667, 1267, doi: [10.1086/519987](https://doi.org/10.1086/519987)

- Strassmeier, K. G., Ilyin, I., Järvinen, A., et al. 2015, *Astronomische Nachrichten*, 336, 324, doi: [10.1002/asna.201512172](https://doi.org/10.1002/asna.201512172)
- Strassmeier, K. G., Ilyin, I., Weber, M., et al. 2018, in *Society of Photo-Optical Instrumentation Engineers (SPIE) Conference Series*, Vol. 10702, *Ground-based and Airborne Instrumentation for Astronomy VII*, ed. C. J. Evans, L. Simard, & H. Takami, 1070212, doi: [10.1117/12.2311627](https://doi.org/10.1117/12.2311627)
- Suárez-Andrés, L., González Hernández, J. I., Israelian, G., Casares, J., & Rebolo, R. 2015, *MNRAS*, 447, 2261, doi: [10.1093/mnras/stu2612](https://doi.org/10.1093/mnras/stu2612)
- Sugar, J., & Corliss, C. 1985, *Atomic energy levels of the iron-period elements: Potassium through Nickel*
- Sukhbold, T., Ertl, T., Woosley, S. E., Brown, J. M., & Janka, H. T. 2016, *ApJ*, 821, 38, doi: [10.3847/0004-637X/821/1/38](https://doi.org/10.3847/0004-637X/821/1/38)
- Suwa, Y., Yoshida, T., Shibata, M., Umeda, H., & Takahashi, K. 2018, *MNRAS*, 481, 3305, doi: [10.1093/mnras/sty2460](https://doi.org/10.1093/mnras/sty2460)
- Sweeney, D., Tuthill, P., Sharma, S., & Hirai, R. 2022, *MNRAS*, 516, 4971, doi: [10.1093/mnras/stac2092](https://doi.org/10.1093/mnras/stac2092)
- Takahashi, K., Yoshida, T., & Umeda, H. 2013, *ApJ*, 771, 28, doi: [10.1088/0004-637X/771/1/28](https://doi.org/10.1088/0004-637X/771/1/28)
- The pandas development Team. 2024, *pandas-dev/pandas: Pandas, v2.2.2*, Zenodo, doi: [10.5281/zenodo.3509134](https://doi.org/10.5281/zenodo.3509134)
- Thorne, A. P., Pickering, J. C., & Semeniuk, J. 2011, *ApJS*, 192, 11, doi: [10.1088/0067-0049/192/1/11](https://doi.org/10.1088/0067-0049/192/1/11)
- Townsley, D. M., Miles, B. J., Shen, K. J., & Kasen, D. 2019, *ApJL*, 878, L38, doi: [10.3847/2041-8213/ab27cd](https://doi.org/10.3847/2041-8213/ab27cd)
- Tucker, M. A., Shappee, B. J., Huber, M. E., et al. 2022, *PASP*, 134, 124502, doi: [10.1088/1538-3873/aca719](https://doi.org/10.1088/1538-3873/aca719)
- van der Walt, S., Colbert, S. C., & Varoquaux, G. 2011, *Computing in Science and Engineering*, 13, 22, doi: [10.1109/MCSE.2011.37](https://doi.org/10.1109/MCSE.2011.37)
- van Roestel, J., Kupfer, T., Green, M. J., et al. 2022, *MNRAS*, 512, 5440, doi: [10.1093/mnras/stab2421](https://doi.org/10.1093/mnras/stab2421)
- Vines, J. I., & Jenkins, J. S. 2022, *MNRAS*, 513, 2719, doi: [10.1093/mnras/stac956](https://doi.org/10.1093/mnras/stac956)
- Virtanen, P., Gommers, R., Oliphant, T. E., et al. 2020, *Nature Methods*, 17, 261, doi: [10.1038/s41592-019-0686-2](https://doi.org/10.1038/s41592-019-0686-2)
- Wall, R. E., Kilic, M., Bergeron, P., & Leiphart, N. D. 2023, *MNRAS*, 523, 4067, doi: [10.1093/mnras/stad1699](https://doi.org/10.1093/mnras/stad1699)
- Wang, B., Zhou, W. H., Zuo, Z. Y., et al. 2017, *MNRAS*, 464, 3965, doi: [10.1093/mnras/stw2646](https://doi.org/10.1093/mnras/stw2646)
- Wheeler, A. J., Abruzzo, M. W., Casey, A. R., & Ness, M. K. 2023, *AJ*, 165, 68, doi: [10.3847/1538-3881/acaad](https://doi.org/10.3847/1538-3881/acaad)
- Wheeler, A. J., Casey, A. R., & Abruzzo, M. W. 2024, *AJ*, 167, 83, doi: [10.3847/1538-3881/ad19cc](https://doi.org/10.3847/1538-3881/ad19cc)
- Whelan, J., & Iben, Icko, J. 1973, *ApJ*, 186, 1007, doi: [10.1086/152565](https://doi.org/10.1086/152565)
- Wiese, W. L., Smith, M. W., & Glennon, B. M. 1966, *Atomic transition probabilities. Vol.: Hydrogen through Neon. A critical data compilation*, ed. Wiese, W. L., Smith, M. W., & Glennon, B. M. (US Government Printing Office)
- Wood, M. P., Lawler, J. E., Sneden, C., & Cowan, J. J. 2013, *ApJS*, 208, 27, doi: [10.1088/0067-0049/208/2/27](https://doi.org/10.1088/0067-0049/208/2/27)
- . 2014, *ApJS*, 211, 20, doi: [10.1088/0067-0049/211/2/20](https://doi.org/10.1088/0067-0049/211/2/20)
- Woosley, S. E. 2019, *ApJ*, 878, 49, doi: [10.3847/1538-4357/ab1b41](https://doi.org/10.3847/1538-4357/ab1b41)
- Yamaguchi, N., El-Badry, K., Rees, N., et al. 2024a, *arXiv e-prints*, arXiv:2405.06020, doi: [10.48550/arXiv.2405.06020](https://doi.org/10.48550/arXiv.2405.06020)
- Yamaguchi, N., El-Badry, K., Fuller, J., et al. 2024b, *MNRAS*, 527, 11719, doi: [10.1093/mnras/stad4005](https://doi.org/10.1093/mnras/stad4005)
- Yang, J., Laycock, S. G. T., Christodoulou, D. M., et al. 2017, *ApJ*, 839, 119, doi: [10.3847/1538-4357/aa6898](https://doi.org/10.3847/1538-4357/aa6898)
- Yi, T., Gu, W.-M., Zhang, Z.-X., et al. 2022, *Nature Astronomy*, 6, 1203, doi: [10.1038/s41550-022-01766-0](https://doi.org/10.1038/s41550-022-01766-0)
- Zahn, J. P. 1977, *A&A*, 57, 383
- Zhang, L., Ge, H., Chen, X., & Han, Z. 2024, *arXiv e-prints*, arXiv:2406.13146, doi: [10.48550/arXiv.2406.13146](https://doi.org/10.48550/arXiv.2406.13146)
- Zheng, L.-L., Sun, M., Gu, W.-M., et al. 2023, *Science China Physics, Mechanics, and Astronomy*, 66, 129512, doi: [10.1007/s11433-023-2247-x](https://doi.org/10.1007/s11433-023-2247-x)
- Zorotovic, M., & Schreiber, M. 2022, *MNRAS*, 513, 3587, doi: [10.1093/mnras/stac1137](https://doi.org/10.1093/mnras/stac1137)
- Zorotovic, M., Schreiber, M. R., Gänsicke, B. T., & Nebot Gómez-Morán, A. 2010, *A&A*, 520, A86, doi: [10.1051/0004-6361/200913658](https://doi.org/10.1051/0004-6361/200913658)